

Journal: 10237
Article: 457



Author Query Form

**Please ensure you fill out your response to the queries raised below
and return this form along with your corrections**

Dear Author

During the process of typesetting your article, the following queries have arisen. Please check your typeset proof carefully against the queries listed below and mark the necessary changes either directly on the proof/online grid or in the 'Author's response' area provided below

Query	Details required	Author's response
1.	Please confirm the inserted city name is correct and amend if necessary.	
2.	Please provide complete details for Ref. ASTM-International (2009).	
3.	Please check and confirm the article title for Ref. Raghavan et al. (1996).	
4.	Please check and confirm the inserted citation of Table 2 is correct. If not, please suggest an alternative citation. Please note that tables should be cited in sequential order in the text.	

On the mechanical behaviour of carotid artery plaques: the influence of curve-fitting experimental data on numerical model results

John J. Mulvihill · Michael T. Walsh

Received: 17 September 2012 / Accepted: 14 November 2012
© Springer-Verlag Berlin Heidelberg 2012

Abstract Computational models of diseased arteries are advancing rapidly, and a need exists to develop more accurate material models of human atherosclerotic plaques. However, intact samples for in vitro mechanical testing are not readily available. Most plaque samples are harvested from carotid endarterectomies where the geometries are not suitable for the boundary parameters necessary for classical uniaxial tensile testing. Experimental studies of biological tissue, particularly human plaque tissue, have not specified the minimum width-to-length (WL) ratio necessary for appropriate tensile testing. This study proposes either tensile or planar shear testing on whole specimen samples depending on the WL ratio. However, a “grey-area” of WL ratios exists which are unsuitable for either test, between 0.5:1 and 4:1 WL ratio. Eighteen plaque samples are investigated in this study, and according to classical approaches, two of the plaque samples have WL ratios suitable for tensile testing and four are suitable for planar shear testing. The remaining twelve samples fall in the grey-area of WL ratio. The study analyses which test method is suitable for the samples in this grey-area and what effect using the incorrect test method has on results from a computational model. The study highlights that tissues above a WL ratio of 2:1 are suitable for planar shear testing, and samples below 1:1 are more suited for tensile testing. Therefore, the “grey-area” can be reduced with certain limitations

applied by the minor strain assumption which need to be taken into account during experimental testing. This study also demonstrates the influence of curve-fitting experimental results using tensile- and planar shear-based boundary parameters from eighteen plaque samples.

Keywords Carotid artery disease · Plaque properties · Mechanical characterisation · Modelling approaches

1 Introduction

Stroke is a sudden necrosis of brain cells caused by an interruption of normal perfusion to the brain. Stroke has the potential to cause irreversible damage to an array of neurological functions in 22–25 % of victims and death within one year for 25 % of victims (Medtech-Insight 2011). One of the main instigators of a stroke event is the presence of atherosclerotic plaque in the carotid arteries (Guyton 1991). Atherosclerosis refers to a condition in which the walls of an artery thicken due to an accumulation of fatty deposits consisting mainly of lipid and connective tissue matrix. Over time, these deposits harden and form a fibrous cap which can rupture and cause an occlusive thrombosis reaction that can prevent normal blood flow to the brain and lead to a stroke event. Carotid artery stenting (CAS) is a minimally invasive technique of mechanically widening a diseased carotid artery, by deploying a stent at the site of stenosis, compressing the atherosclerotic plaque and widening the lumen to increase blood perfusion. Despite the numerous advantages of CAS over carotid endarterectomy such as increased accessibility, decreased trauma and absence of general anaesthetic (Roffi et al. 2009), it accounts for only 26 % of stroke prevention procedures performed due to the lack of knowledge on the mechanical effect of stents on the plaque structure (Paraskevas et al. 2009).

EMBARK Initiative from the Irish Research Council, Dublin 4, Ireland.

J. J. Mulvihill · M. T. Walsh (✉)
Department of Mechanical, Aeronautical and Biomedical Engineering,
CABER Centre for Applied Biomedical Engineering, Materials and
Surface Science Institute, University of Limerick, Limerick, Ireland
e-mail: michael.walsh@ul.ie

J. J. Mulvihill
e-mail: john.mulvihill@ul.ie

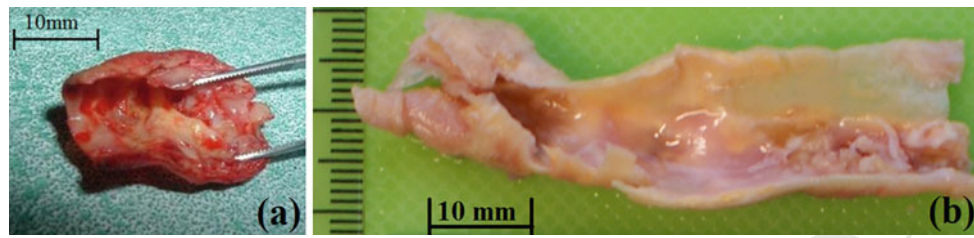


Fig. 1 **a** Fresh whole specimen CAP from the Lawlor et al. (2011) study and **b** a defrosted sample from an ongoing study which highlights the variability in plaque geometry, material and location in the artery

57 Computational studies of atherosclerotic arteries under
 58 physiological conditions have evaluated the stress distribution
 59 within the plaques to analyse the biomechanical response to
 60 certain geometrical, structural and material variations (Li et
 61 al. 2008; Kioussis et al. 2009; Creane et al. 2010; Franquet
 62 et al. 2011). A limited number of studies have also exam-
 63 ined the biomechanical structural alterations of the plaque
 64 to the deployment of stents to improve the design of the
 65 stent (Takashima et al. 2007; Cui et al. 2010; Auricchio et
 66 al. 2011; Scherer et al. 2011). Computational studies of dis-
 67 eased coronary arteries are more common than the carotid
 68 (Cilla et al. 2012; Huang et al. 2001; Versluis et al. 2006)
 69 and a main limitation in these studies is the material proper-
 70 ties representing the plaque model which are developed from
 71 experimental data based on a small sample size of human
 72 plaque from the aorta (Beattie et al. 1998; Lendon et al. 1993;
 73 Loree et al. 1994a), limiting the reliability of the stress values
 74 from these studies. The computational simulations of dis-
 75 eased carotid arteries also base the material properties of the
 76 carotid plaque on experimental data of atherosclerosis from
 77 other parts of the vasculature which have different morphol-
 78 ogies and potentially different mechanical responses to stent
 79 deployment (Herisson et al. 2011), excluding Creane et al.
 80 (2010) which is based on uniaxial tensile data of fresh human
 81 carotid plaques undertaken by Maher et al. (2009).

82 Ideally for improved material properties of diseased tissue,
 83 in vivo mechanical characterisation of carotid atherosclerotic
 84 plaque (CAP) would be carried out on a patient to develop
 85 a specific constitutive material model and apply it to their
 86 diseased artery geometry. However, there is no fully vali-
 87 dated method of carrying out this in vivo mechanical char-
 88 acterisation procedure. Current studies that mechanically
 89 characterise CAPs use in vitro mechanical test procedures
 90 developed for engineering materials with specific geometry
 91 requirements to satisfy the minor strain assumptions such
 92 as pure tension and equi-biaxial testing. Limitations when
 93 mechanically characterising any type of excised intact plaque
 94 tissue are the random geometry and variance in mechanical
 95 response, making it difficult to test the CAP specimen as a
 96 whole in pure tension (a common test method for mechan-
 97 ically characterising biological tissue when using a strain
 98 energy function (SEF)). Figure 1 highlights the geometrical

99 difference between CAPs excised after a carotid endarterec-
 100 tomy, Fig. 1a is from Lawlor et al. (2011) which is a fresh
 101 human CAP tested immediately after excision from the com-
 102 mon carotid. Figure 1b is a defrosted human CAP from the
 103 carotid bifurcation (left-side) through to the common carotid.
 104 There are many limitations to in vitro mechanical character-
 105 isation of biological tissue such as the deleterious effect on
 106 the structure and residual stresses within the plaque during
 107 excision, damage to tissues from clamping and inhomogene-
 108 ity of the CAP tissue material for an ideal failure at the centre
 109 of the specimen.

110 In vitro studies, testing human and animal biological tis-
 111 sue in tension, range the width-to-length (WL) ratio from
 112 0.5:1 to 0.167:1 in both the circumferential and longitudinal
 113 directions, Table 1 (excluding ASTM-International (2009)
 114 which is a standard based on engineering materials). Specif-
 115 ically examining the studies of human plaque, the WL ratio
 116 varies from 0.3:1 to 0.21:1. The shortest gauge lengths used in
 117 these tensile test studies were 3 and 4 mm, Richardson (2002)
 118 and Maher et al. (2009), respectively, where it was stated
 119 that such a small distance between the clamps can affect the
 120 stress distribution within the material during testing. Exclud-
 121 ing this gauge length, the experimental plaque studies range
 122 from 7 to 15.9 mm in gauge length where in theory this
 123 length should be much longer to allow for a larger uniform
 124 stress distribution for the governing equations of major and
 125 minor strains to hold true when applying the experimental
 126 data to a SEF. However, as the tissue contains interconnected
 127 fibres, this cutting can deleteriously affect the structure of
 128 the fibres as well as alter the global mechanical properties
 129 of the plaque. For an immediate improvement in the consti-
 130 tutive material models of CAPs, it is necessary to mechan-
 131 ically characterise the whole plaque specimen as separating
 132 the specimen into smaller sections can potentially underes-
 133 timate the global mechanical properties (Lawlor et al. 2011;
 134 Borschel et al. 2003).

135 Due to the nature of the CAP geometry, when excised
 136 from the artery, this study investigates the limitations that
 137 geometric ratios associated with excised plaque specimens
 138 (WL ratios) have when mechanically tested in either pure ten-
 139 sion or planar shear. A “grey-area” of unsuitable WL ratios
 140 is created between the correct ratios for tensile and planar

Table 1 List of experimental studies using tensile tests on biological tissue which also detail the gauge lengths and widths of the samples tested

Author	Length (mm)	WL	Tissue type
Stemper et al. (2005)	15.9	0.5:1	Human carotid artery
Lally et al. (2004)	9.38	0.37:1	Porcine coronary artery
Hanuza et al. (2010)	30	0.33:1	Human aortic artery
Holzapfel et al. (2004)	7–17	0.31–0.13:1	Human iliac plaque
Loree et al. (1994a)	15.9	0.3:1	Human aortic plaque
Raghavan et al. (1996)	40	0.25:1	Human aortic aneurysm
Wang et al. (2001)	40	0.25:1	Human aortic thrombus
ASTM E8	N/A	0.25:1	Tensile testing standard
Maher et al. (2009)	4	0.25:1	Human carotid plaque
Xiong et al. (2008)	20–25	0.25–0.2:1	Human aortic aneurysm
Teng et al. (2009)	9	0.22:1	Human carotid plaque
Lendon et al. (1993)	7	0.21:1	Human aortic plaque
Silver et al. (2003)	10	0.2:1	Porcine carotid artery
Guinea et al. (2010)	10	0.2:1	Human aortic artery
Di Martino et al. (1998)	22	0.2:1	Human aortic artery
Veronda et al. (1970)	45.7	0.167:1	Cat skin
Richardson (2002)	3	0.167:1	Human coronary plaque

Table 2 List of WL ratios used in a number of experimental studies using mechanical tests on biological tissue in planar shear

Author	Length (mm)	WL	Tissue type
Davis (2004)	N/A	4:1	Shear standard
Gao et al. (2009)	11	4.6:1	Porcine liver
Hollenstein et al. (2011)	10	6:1	Porcine skin

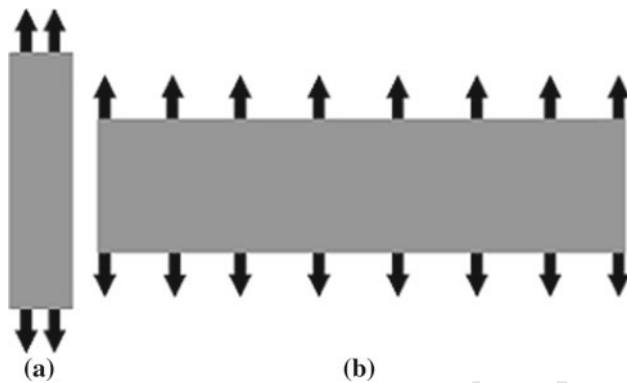


Fig. 2 Idealised computational models of tensile and planar shear uniaxial tests. **a** WL 0.25:1 suitable for tensile testing and **b** WL 4:1 suitable for planar shear testing

planar shear tests for 18 carotid plaques, on a computational model of an idealised stenosed carotid artery. An understanding of the limitations and percentage error from theoretical minor strains for CAP samples in the grey-area will aid in improved experimental methods when testing whole CAP specimens and more accurate constitutive material models (Table 2).

2 Materials and methods

2.1 Ratio analysis

A computational analysis of the stresses in a test specimen with varying geometric ratio (WL 0.1:1–10:1) was carried out with a consistent hyperelastic material property. By examining the effect of the WL ratio on the resolved stresses and minor strain of the test specimens, the errors involved when the WL ratio is in the “grey-area” for suitable mechanical testing, 0.5:1 to 4:1, were identified. Figure 2 illustrates two of the twelve computational models employed in this study. Figure 2a shows an ideal geometry for tensile testing with a WL ratio of 0.25:1, (b) illustrates a model with a WL ratio of 4:1 suitable for planar shear testing. Comparison of the minor strain at the centre of gauge length

shear testing. Currently this “grey-area” is between WL 0.5:1 and 4:1 according to Davis (2004). Unfortunately for whole specimen testing of CAP tissue excised from carotid endarterectomies, the sample geometry can fall into this area. Therefore, there is a need to investigate the feasibility of reducing this area and investigate the errors involved when testing inside this “grey-area”. These findings will aid in understanding the effect of changing the governing equations of principal stretches, to suit either tensile or

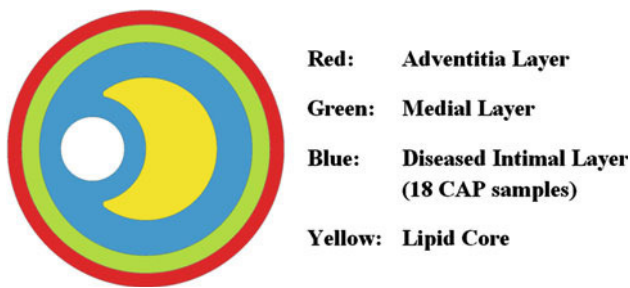


Fig. 3 Dimensioned diagram of the idealised 2D planar model of a diseased carotid artery

of each geometric ratio to the theoretical minor strain will highlight in an idealised computational uniaxial setup the errors involved for geometric ratios within the “grey-area” of 0.5:1–4:1 WL ratios. The “grey-area” is the range of WL ratios which are theoretically unsuitable for tensile or planar shear testing for engineering materials. However, for whole specimen biological tissue testing, this grey-area is too large and needs to be redefined to a smaller range as the current area significantly reduces the number of samples suitable for testing.

2.2 Idealised diseased artery

A two-dimensional cross-section of an idealised atherosclerotic artery was modelled using geometries analogous to work carried out by Li et al. (2008) and Franquet et al. (2011). The geometric model contains a large lipid core which is surrounded by a diseased intimal layer with a fibrous cap of 0.6 mm, Fig. 3. The internal diameter of the artery is 6 mm which was based on Franquet et al. (2011) and reiterated in experimental work by Krejza et al. (2006). The lumen diameter was chosen to be 30% of the artery diameter, 1.8 mm, which is based on the typical minimum stenosis of a diseased artery which undergoes carotid endarterectomy. The 0.9 mm thickness of the carotid wall was based on Delfino et al. (1997), but can vary up to 1.5 mm (Li et al. 2008). The artery wall was divided into the medial and adventitial layers according to Holzapfel et al. (2000), 0.4 and 0.5 mm, respectively. The lipid core size and shape were based on Franquet et al. (2011). A peak physiological systolic pressure value of 18 kPa was applied uniformly to the wall of the lumen for each model (Cilla et al. 2012).

Grid independence was established using a 6-noded free triangular mesh applied throughout the whole finite element (FE) model. Hybrid formulation, used for incompressible and large deformation problems, and plane strain were applied to this model. Elements were concentrated around the lumen and fibrous cap region, but with at least 6 elements through the thickness of the medial and adventitial layer.

2.3 Material properties

The CAP properties were based on the experimental data of fourteen CAP samples from Lawlor et al. (2011) as well as data of four CAP samples from that study which were not included due to the unsuitability of the WL ratios for tensile testing. The stress-strain data of each plaque were fitted to a third-order reduced polynomial SEF, the Yeoh form, using an optimisation technique developed with Matlab (r2009a, Natick, MA; The Mathworks Inc., 2009) to minimise the difference in stress values between the Yeoh SEF and the experimental data. The optimisation technique was carried out for each CAP sample using both tensile and planar shear principal stretches leaving 36 material models in the numerical study.

$$\Psi(I_1) = \sum_{(i=1)}^3 C_{i0}(I_1 - 3)^i \quad (1)$$

The Yeoh SEF is suitable for characterising hyperelastic materials using uniaxial mechanical data, in tension or planar shear, as the function does not depend on the second strain invariant of the Cauchy Green deformation tensor, I_2 . C_{i0} are the material coefficients, and I_1 is the first-strain invariant which is based on the principal stretch ratios, Eq. 2.

$$I_1 = \lambda_1^2 + \lambda_2^2 + \lambda_3^2 \quad (2)$$

The principal stretches (λ_1 , λ_2 and λ_3) change depending on the uniaxial test, tensile or planar shear, where in both cases λ_1 is the stretch in the loading direction. For tensile testing, the principal stretches are:

$$\lambda_1 = \lambda, \lambda_2 = \lambda_3 = \frac{1}{\sqrt{\lambda}} \quad (3)$$

For planar shear testing:

$$\lambda_1 = \lambda, \lambda_2 = 1, \lambda_3 = \frac{1}{\lambda} \quad (4)$$

The WL ratio governs the degree of deformation that the minor stretch ratio component (λ_2) undergoes during a tensile or planar shear test. During a planar shear test, the minor principal stretch ratio (λ_2) is considered to be 1 which equates to zero strain in the transverse direction. According to Davis (2004), the minor strain is 0.05 times the major strain when the WL ratio is 4:1 which is close to the plane strain condition necessary for the test (Palmieri et al 2009). However, any WL ratio lower than this can lead to a larger deviation from the zero strain assumption in the minor direction. For tensile testing, the minor axis experiences compressive, negative strains, as the principal strain is positive. This study developed two constitutive material models for each of the eighteen plaques based on the Yeoh form, using the tensile and planar shear boundary parameters, and analysing

Table 3 List of the SEF parameters used for the adventitial and medial layers in this study taken from Cilla et al. (2012)

Layer	μ (kPa)	k_1 (kPa)	k_2 (kPa)	κ
Adventita	8.44	547.67	568.01	0.26
Media	1.4	206.16	58.55	0.29

Table 4 List of gauge length, WL ratios and plaque type for each CAP sample

Plaque	Length (mm)	WL	Type
1	16	1.19:1	Mixed
2	7.8	2.25:1	Soft
3	4.72	3.51:1	Soft
4	5.8	0.45:1	Mixed
5	3.1	5.55:1	Mixed
6	7.98	1.04:1	Hard
7	10.05	1.32:1	Soft
8	3.96	5.02:1	Soft
9	6.1	1.93:1	Hard
10	5.6	2.55:1	Soft
11	6.42	2.02:1	Mixed
12	6.11	2.05:1	Soft
13	5.18	2.53:1	Soft
14	4.57	0.44:1	Mixed
15	6.89	4.50:1	Mixed
16	7.08	1.90:1	Mixed
17	2.88	4.01:1	Soft
18	9.89	1.95:1	Mixed

the effect that the WL ratio can have on the stress distribution and mechanical response in an idealised FE model. The lipid core was based on Akyildiz et al. (2011), where the lipid core is treated as a very soft and nearly incompressible tissue, with a Young’s Modulus of 1 kPa and Poisson’s ratio of 0.45 rather than an incompressible liquid, which is based on experimental work carried out by Loree et al. (1994b). Other approaches (Loree et al. 1994b) have treated the lipid core as a nearly incompressible fluid which is not able to sustain shear stress. The effects of the 1 kPa assumption on the trends presented in this study were evaluated and discussed in the limitations section. The arterial media and adventitia layers were modelled using an anisotropic SEF developed by Gasser et al. (2006). The strain energy per unit of reference volume is represented as Ψ .

$$\Psi = \mu(I_1 - 3) + \frac{k_1}{k_2} (\exp(k_2[\kappa(I_1 - 3) + (1 - 3\kappa)(I_4 - 1)]^2) - 1) \tag{5}$$

From Eq. 5, μ , k_1 , k_2 and κ are material parameters, I_1 and I_4 are invariants of the Cauchy Green strain tensor. The parameter kappa ($0 \leq \kappa \leq 1/3$) describes the level of dispersion in the fibre directions. The parameters for adventitial and medial layers were based on readily available data of arterial tissue from Cilla et al. (2012), listed in Table 3. The model was assumed incompressible, by setting the compressibility value (D) to zero for each material property, to simplify the material model (Holzapfel et al. 2000).

3 Results

3.1 Ratio analysis

Table 4 lists the different gauge lengths, WL ratios and plaque type of the CAP samples tested, highlighting the size and random nature of the CAP specimens. Figure 4 illustrates the percentage error of the minor strains of each WL ratio, from 0.1:1 to 10:1, from the theoretical minor strain suitable for either tensile (red area) or planar shear (blue area) testing. For example, any WL ratio less than 0.5:1 has minor strain values 100% in error for planar shear testing and WL ratios greater than 4:1 has minor strain values 100% in error for

tensile testing making any of these ratios unsuitable for those test methods.

Using current standard approaches and the WL ratios in Table 4, only two CAP samples are suitable for tensile testing (4 and 14) and four CAP samples are suitable for planar shear testing (5, 8, 15 and 17) leaving twelve CAP samples unsuitable for either test. Excluding twelve CAP samples from this experimental study is not ideal due to the difficulty of acquiring these human CAP samples and the desire not to deleteriously cut the samples into smaller sections which could significantly alter the global mechanical properties. Therefore, it was decided to assess the current “grey-area” WL ratios to determine the theoretical minor strain errors involved with test samples in this area.

FE analysis of WL ratios from 0.1:1 to 10:1 shows that ratios less than 0.5:1 and greater than 4:1 are suitable for tensile and planar shear testing, respectively, as the minor strain is correct within 5% for more than 80% of the gauge length, Fig. 5c, d. However, for the ratios that fall between 0.5:1 and 4:1, the minor strains are less than 80% of the gauge length, Fig. 5a, b (1:1 and 2:1, respectively). From Fig. 4, the percentage error from the theoretical minor strain of 2:1 WL is 65 and 32% from tension and planar shear, respectively, indicating that planar shear testing is more suitable. However, this is only true for 55% of the gauge length area, Fig. 5b. Again looking at Fig. 4 for the WL ratio 1:1, the percentage error is 12 and 85% from tension and planar shear, respectively, indicating that tensile testing is more suitable.

Fig. 4 The percentage error of each CAP sample (black X) from the theoretical minor strain suitable for tensile (dark red line) and planar shear (dark blue line) for each geometric ratio that is suitable for tension (0.1:1–0.5:1), for planar shear (4:1–10:1) and in the “grey-area” (0.5:1–4:1)

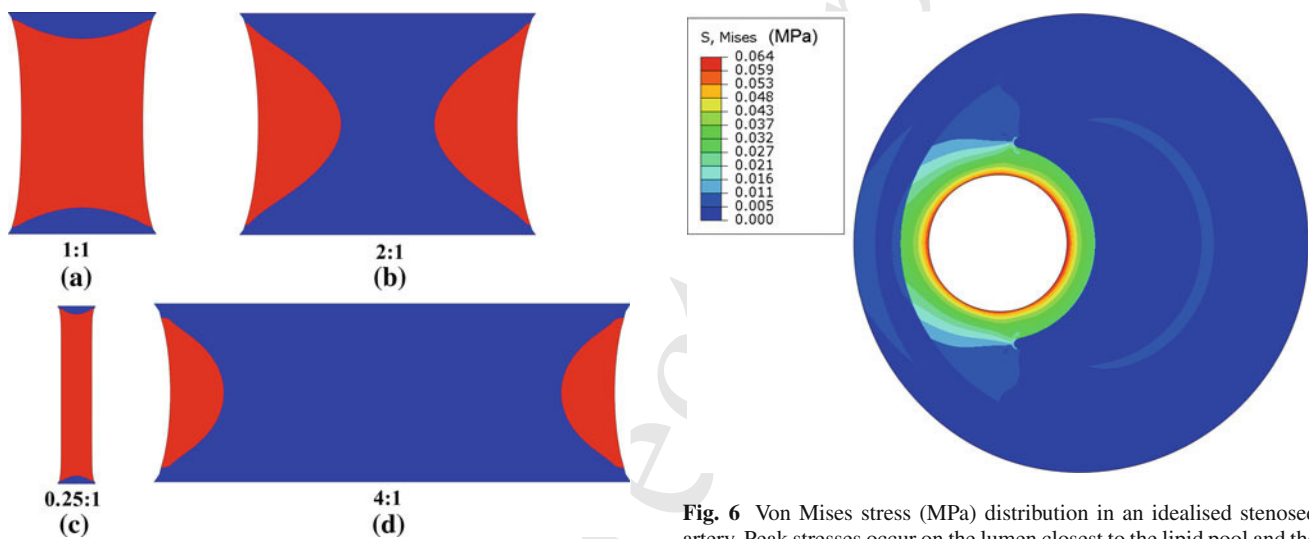
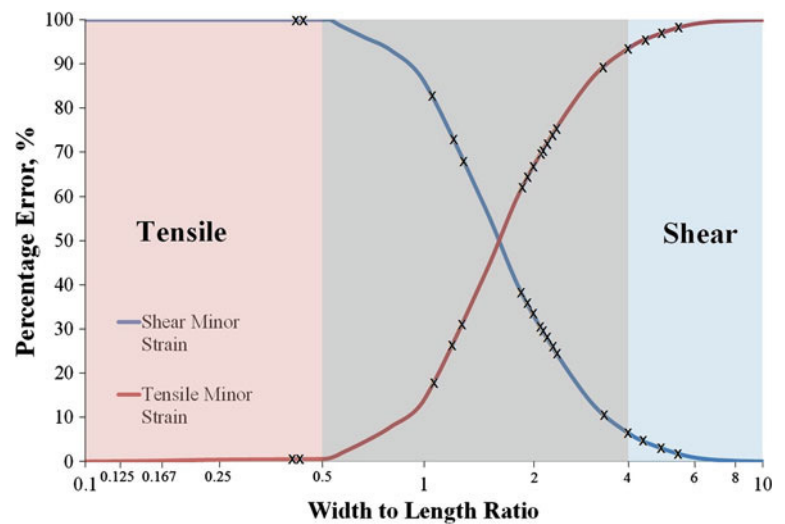


Fig. 5 Minor Strain plots for tension and planar shear of samples with different WL ratios: **a** 1:1, **b** 2:1, **c** 1:1 and **d** 4:1, where red denotes minor strain suitable for tension (**a**, **c**) and blue is suitable for planar shear (**b**, **d**)

Fig. 6 Von Mises stress (MPa) distribution in an idealised stenosed artery. Peak stresses occur on the lumen closest to the lipid pool and the shoulder regions of the lipid pool

were typically larger in the FE models using the planar shear-based SEF.

Figure 7 quantitatively shows the difference in radial displacement from the lumen centre along a horizontal centreline through the stenosed artery model. This graph highlights the similar behaviour of both models, but the larger radial displacement of the planar shear SEF through each section of the model of CAP sample 8. Figure 8 illustrates the difference in peak radial displacement between the tensile-based SEF model (a) and the planar shear model (b) of CAP sample 8 where the planar shear model has larger displacements for this particular sample and for all samples, excluding sample 6. CAP sample 8 was chosen as the geometry of the specimen suggested that it should be characterised in planar shear rather than tension, and the sample best illustrates the underestimation in radial displacement for a tensile-based FE model shown in Fig. 8a.

319 However, again this is only true for 70% of the gauge length,
320 Fig. 5a.

321 3.2 Idealised diseased artery

322 An example of the von Mises stress distribution of a 2D plane
323 strain-idealised diseased artery model is shown in Fig. 6,
324 CAP sample 7, using material model developed from planar
325 shear principal stretches (Eq. 4). The peak von Mises stress
326 typically occurs at the point on the lumen closest to the lipid
327 pool. The peak von Mises, maximum principal stresses and
328 radial displacement were recorded. A constitutive model was
329 developed for each of the CAP samples in both tension and
330 planar shear, based on Eqs. 3 and 4, respectively. The results
331 demonstrated that the peak stress and displacement values

Figures 9, 10 and 11 are data plots of the radial displacements along the circumference of the lumen, where the start point (0°) is at the right side of the lumen closest to the lipid core and continues counter clockwise. These figures compare the radial displacement of the undeformed original lumen to the deformed lumen of both the tensile and planar shear models of CAP samples 8, 14 and 13, respectively. CAP samples 8 and 14 were chosen as the WL ratios of each are suitable for planar shear and tension, respectively. CAP sample 13 has a WL ratio of 2.53:1 which places the sample in the grey-area and creates a reduced percentage difference in lumen area between the planar shear and tension.

Each of the CAP samples were assigned to averaged WL ratios, which ranges from 0.5:1 (suitable for tensile testing) to 5:1 (suitable for planar shear) in increments of 1, and the percentage difference of the radial displacements of the lumen area between the tensile and planar shear models were analysed in Fig. 12. Figure 12 highlights that the percentage

difference between the tensile and planar shear models of each CAP sample is higher at the WL ratios suitable for tensile, 0.5:1, and planar shear, 4:1 and 5:1. This suggests that reassessing the “grey-area” can alter the WL ratios limits to a maximum of WL 1:1 for tensile testing and a minimum WL of 2:1 for planar shear where only 6 of the 18 (33%) of the CAP samples are unsuitable for testing, Fig. 13.

4 Discussion

Recent computational studies aim to simulate the deployment of stents in diseased carotid arteries and to evaluate the stress distribution in vivo throughout the plaque. These studies make it imperative to understand the global mechanical properties of carotid plaques. Idealised FE analysis of different WL ratios highlighted the significant errors in the minor strain associated when testing a specimen outside of the suitable ratios for tensile and planar shear testing.

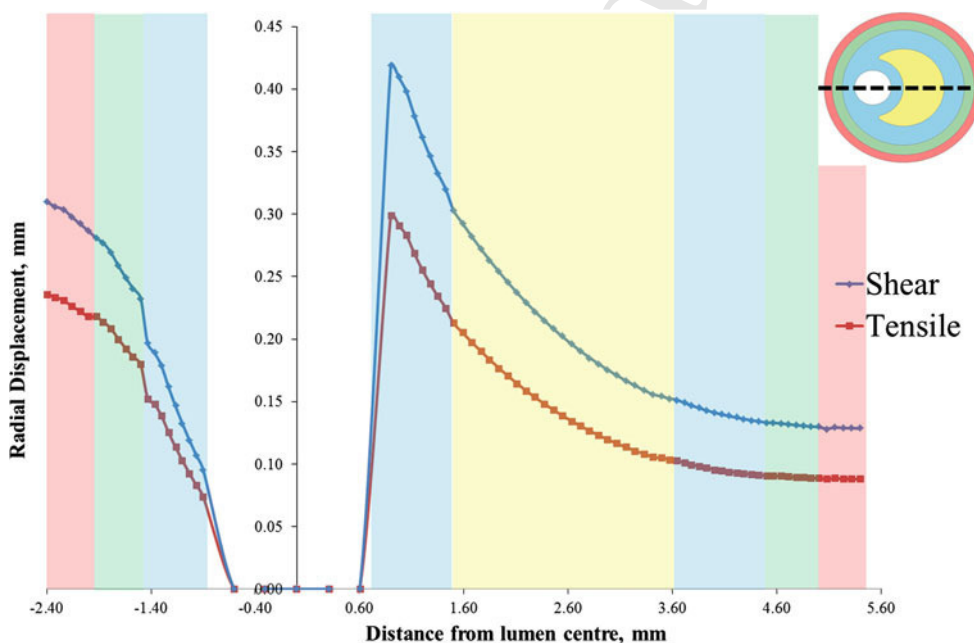
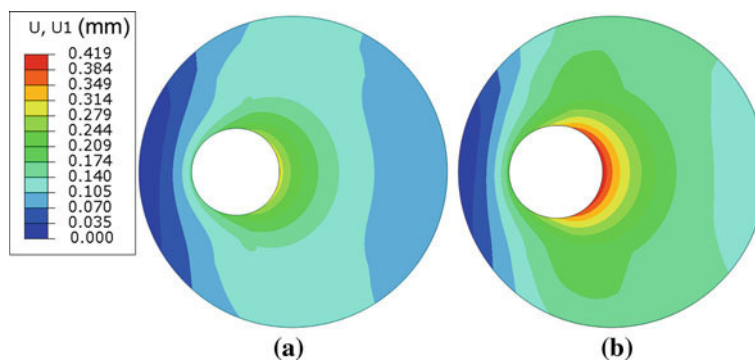


Fig. 7 Radial displacement from lumen centre along dashed line (inset) of stenosed artery for both the tensile (red) and planar shear (blue) models for CAP sample 8. Shaded regions on plot match the material sections outlined in Fig. 3 (inset)

Fig. 8 Contour of radial displacement (mm) from lumen centre in an idealised stenosed model of plaque sample 8 with a material model based on tensile (a) and planar shear (b) principal stretches



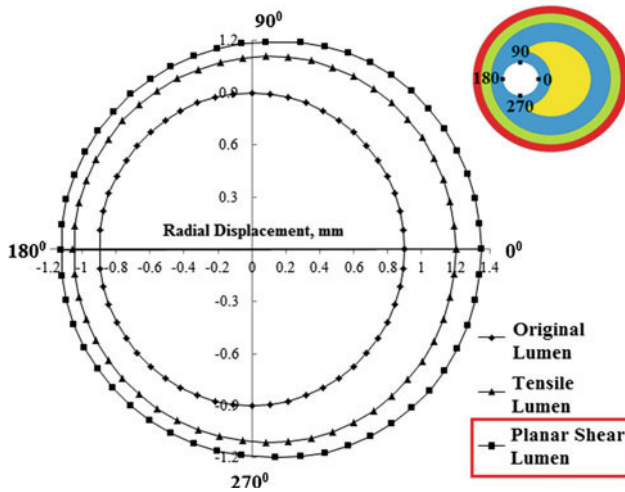


Fig. 9 Radial displacement (mm) along lumen circumference of the original lumen diameter and the deformed lumen for the tensile and planar shear models for CAP sample 8, where the WL ratio (5.02:1) is suitable for planar shear testing, *red box*

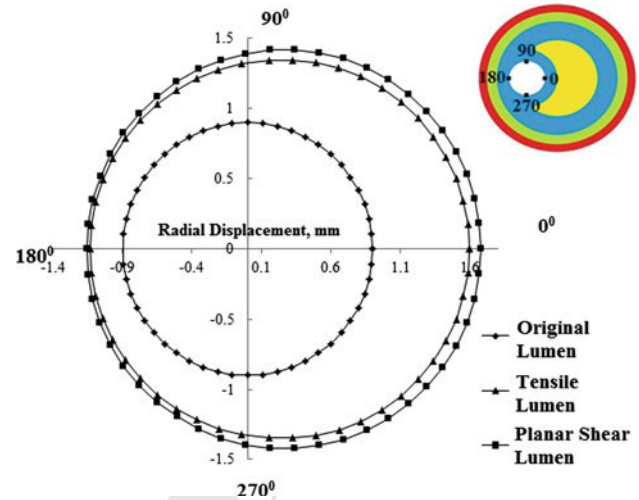


Fig. 11 Radial displacement (mm) along lumen circumference of the original lumen diameter and the deformed lumen for the tensile and planar shear models for CAP sample 13, where the WL ratio (2.53:1) falls in the “grey-area” of testing

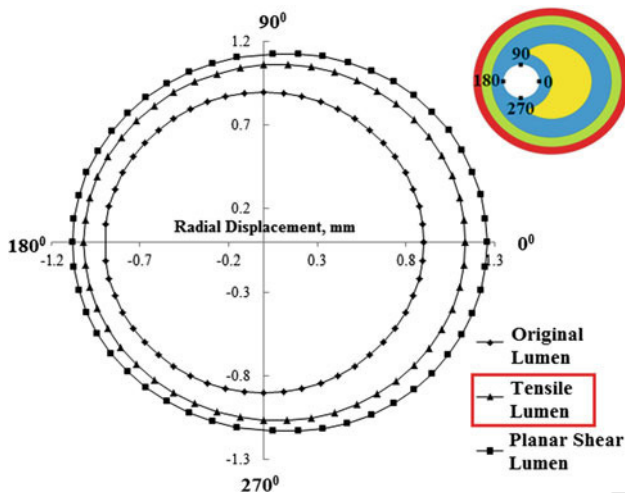


Fig. 10 Radial displacement (mm) along lumen circumference of the original lumen diameter and the deformed lumen for the tensile and planar shear models for CAP sample 14, where the WL ratio (0.44:1) is suitable for tensile testing, *red box*

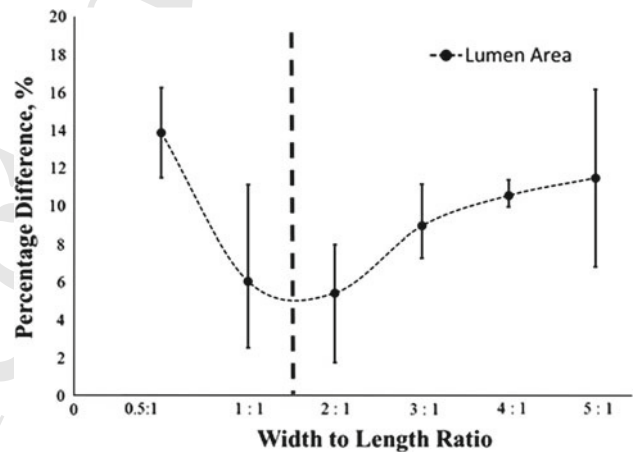


Fig. 12 Percentage difference between lumen areas of material models based on tensile or planar shear principal stretches for each plaque sample (grouped by WL ratio). The dashed line indicates the lowest percentage error and cut-off point between using tensile and planar shear tests

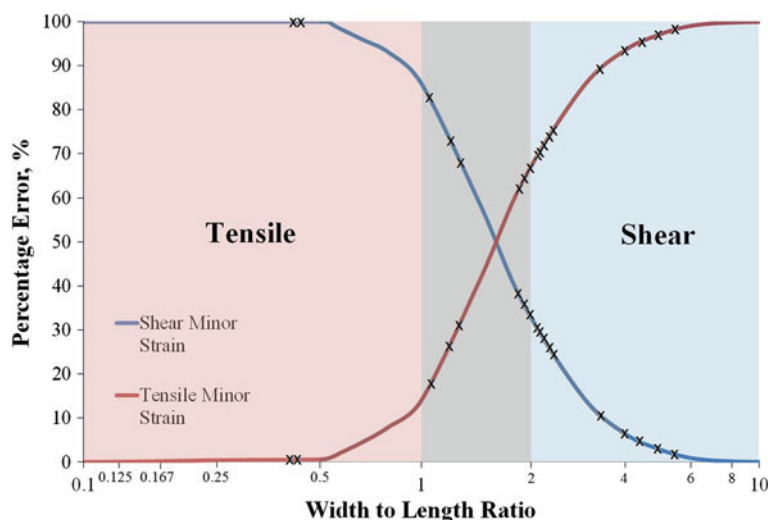
382 Unlike engineering materials, biological tissue cannot be
 383 altered to suit the required geometrical parameters needed
 384 for the boundary conditions to analytically develop constitu-
 385 tive material models, without changing the global mechani-
 386 cal behaviour of the sample. The acquisition of whole human
 387 CAP specimens is difficult and limited which makes it imper-
 388 ative to mechanically test every available specimen even
 389 when the WL ratio does not fall within current standards.
 390 Twelve of the eighteen plaques were theoretically unsuitable
 391 for either tensile or planar shear testing, Table 4. However, a
 392 precise knowledge of the errors involved and a reduction of
 393 this “grey-area” can aid in improved experimental methods

and more accurate material models for FE analysis of stent
 deployment without wastage of CAP samples.

4.1 Ratio analysis

The geometric ratio analysis carried out in this study illus-
 trates the large error in minor strain between WL ratios 0.5:1
 and 4:1 for both tensile and planar shear testing, Fig. 4. This
 analysis highlights the limitation when testing specimens in
 this “grey-area”. However, as twelve of the eighteen plaque
 specimens are in this area, it is a common and unavoidable
 issue. The use of contactless measurement of the strain in an

Fig. 13 The percentage error of each CAP sample (black X) from the theoretical minor strain suitable for tensile (dark red line) and planar shear (dark blue line) where the limits have been reassessed to reduce the “grey-area” from WL 0.5:1–4:1 to WL 1:1–2:1



404 area of the sample where the minor strain is known to be suitable
 405 for pure tension or planar shear throughout the whole
 406 test could improve the accuracy of the results. For example,
 407 WL 2:1 ratio the minor strain at 50 % strain is in planar shear
 408 for only 55 % of the gauge length from the vertical centre,
 409 Fig. 5b, whereas for WL 1:1 ratio the minor strain is correct
 410 for tension in only 70 % of the gauge length at 50 % strain,
 411 Fig. 5a. The contactless strain measurement would have to
 412 take into account this limited area for each ratio in the area
 413 throughout the test. This is necessary to ascertain accurate
 414 global mechanical behaviour of CAP samples for improved
 415 SEF material models to be used in future FE studies.

416 4.2 Idealised diseased artery

417 The computational study on the idealised stenosed artery
 418 evaluated the effect of changing the principal stretches, to
 419 tensile or planar shear, had on the numerical model through
 420 the altered SEF. The peak von Mises stress values typically
 421 occurred at the point on the lumen closest to the lipid core
 422 due to the soft and deformable nature of the core material.
 423 The peak maximum principal stress was located on the
 424 lumen closest to the lipid core for twelve of eighteen (66 %)
 425 samples and at the shoulder cap region of the lipid core for
 426 six of the eighteen (33 %) samples. The difference between
 427 the peak stress at each location was no greater than 12 %
 428 for these CAP models for either the tensile or planar shear
 429 approaches. The peak stress values were typically larger for
 430 the planar shear-based models. The largest deformation of
 431 the lumen occurred in CAP samples 2 and 17 due to the soft
 432 nature of these samples allowing for a large displacement.

433 In theory, the planar shear-based SEF is expected to be
 434 stiffer than the tensile-based version when using the same
 435 experimental data. The results from the numerical model reiterate this theoretical expectation as there is decreased stress

and radial displacement in CAP sample models that should
 be based on planar shear test rather than tensile, Fig. 8. This
 emphasises the incorrect assumption of characterising samples
 in the grey-area that have greater width than length to a
 tensile-based SEF. This assumption can lead to numerical
 models underestimating the realistic global mechanical
 behaviour of the CAP samples with these geometrical ratios,
 Figs. 9, 10 and 11. Figure 10 shows sample 14 which is suited
 for tensile testing only and that the FE model using the planar
 shear-based SEF overestimates the lumen displacement and
 vice versa for Fig. 9.

Assigning the CAP sample models to WL ratios in the
 “grey-area”, which ranges from 0.5:1 (suitable for tensile
 testing) to 4:1 (suitable for planar shear) in increments of 1,
 the greatest percentage error between lumen area occurred at
 the extremities, 0.5:1 and 5:1, as these ratios are farthest
 from the specified geometrical ratio needed for the respective
 test method, Fig. 12. For certain samples between, 1:1 and
 2:1 the percentage difference between the lumen areas is
 reduced; as expected from Fig. 4 the percentage errors are
 similar from tension and planar shear for these WL ratios.
 Results show that characterising experimental data of a CAP
 sample with a geometric ratio unsuitable for either uniaxial
 test to a SEF has a significant effect on the numerical analysis.
 However, as acquisition of human CAP specimens suitable for
 in vitro mechanical testing is limited, it is necessary to
 characterise these particular CAP samples. Prior to this study,
 the “grey-area” was not clearly defined for unsuitable
 geometrical ratios of biological soft tissues for tensile testing
 as some studies used WL ratios as low as 0.4:1, but according
 to engineering standards, the grey-area can be between
 0.25:1 and 4:1.

This study demonstrates that planar shear testing can be
 carried out on samples with WL ratios as low as 2:1 with
 certain errors in the minor strain involved and for samples
 below 1:1 tensile testing is suitable, but again with certain

Author Proof

471 limitations involved for ratios that fall within the “grey-area”.
 472 Therefore, the “grey-area” is reduced from $0.5:1 \leq WL \leq 4:1$
 473 to $1:1 \leq WL \leq 2:1$ (Fig. 13). It is also proposed that if a CAP
 474 sample has a WL ratio that falls within this new “grey-area”
 475 the gauge length should be altered when mounting the spec-
 476 imen in the clamps to achieve a WL ratio outside this “grey-
 477 area” avoiding the larger errors involved and improving the
 478 accuracy of the material model developed to characterise the
 479 CAP sample.

480 4.3 Limitations

481 The simplified computational analysis of the idealised ratios
 482 with uniform thickness was carried out to highlight the errors
 483 these geometric ratios contain when compared to theoret-
 484 ical minor strain. The idealised 2D plane strain models were
 485 used in the numerical study is an over-simplification of a dis-
 486 eased artery. However, as this was a comparative study, this
 487 setup was deemed suitable as was the exclusion of residual
 488 strains and geometrical variations of the CAP samples. The
 489 effects of the 1 kPa assumption on the trends of this study
 490 were evaluated by varying the Young’s Modulus of the lipid
 491 core down to zero and this affected the peak von Mises stress,
 492 peak displacement and deformed lumen area results by 3.33,
 493 6.08 and 1.57 %, respectively. The CAP samples were char-
 494 acterised using the Yeoh SEF which assumes the material
 495 is isotropic and homogenous. However, as the main priority
 496 of this study is to analyse the plaque behaviour in the cir-
 497 cumferential direction, the authors believe that an isotropic
 498 and homogenous assumption for the material properties is
 499 appropriate. This methodology of intact plaque testing is not
 500 without its own limitations, and the authors ultimately wanted
 501 to assess the strength of these tissues as a whole. Biaxial test-
 502 ing of plaque samples is necessary in future studies that aim
 503 to understand the anisotropic behaviour of carotid plaques
 504 (Holzapfel et al. 2004). The sample size of CAPs used in
 505 this study was small, but this limitation further highlights the
 506 need to redefine the ratios grey-area that can be used for uni-
 507 axial testing as well as taking into account the experimental
 508 errors to improve the data needed for curve fitting of SEFs.

509 5 Conclusion

510 This study highlights that using the incorrect boundary param-
 511 eters in a SEF can affect the peak stress and radial displace-
 512 ment values in a numerical model. The percentage error radial
 513 displacement is largest for CAP samples with WL ratios of
 514 $0.5:1$ and $5:1$ between the constitutive models developed for
 515 tensile and planar shear. It is important to characterise the
 516 sample using the correct boundary conditions, tensile or planar
 517 shear, for samples with certain geometrical ratios. How-
 518 ever, as many whole CAP specimens typically do not have

the required geometric ratio to suit these parameters, this
 study suggests to characterise samples to a SEF that have
 a WL ratio of $1:1$ or less using tensile parameters and for
 samples greater than WL $2:1$ to a planar shear setup. There
 are significant limitations when following these assumptions,
 and the use of contactless strain measurement in an area of
 the sample where the minor strain is known to be correct is
 imperative for more accurate experimentation of these CAP
 samples in the grey-area.

References

- Akyildiz A, Speelman L, van Brummelen H, Gutierrez M, Virmani R, van der Lugt A, van der Steen A, Wentzel J, Gijssen F (2011) Effects of intima stiffness and plaque morphology on peak cap stress. *Biomed Eng Online* 10(1):1–13
- ASTM-International (2009) Standard test methods for tension testing of metallic materials
- Auricchio F, Conti M, De Beule M, De Santis G, Verheghe B (2011) Carotid artery stenting simulation: from patient-specific images to finite element analysis. *Med Eng Phys* 33(3):281–289
- Beattie XuC, Vito R, Glagov S, Whang CM (1998) Mechanical analysis of heterogeneous, atherosclerotic human aorta, vol 120. American Society of Mechanical Engineers, New York
- Borschel GH, Kia KF, Dennis RG (2003) Mechanical properties of acellular peripheral nerve. *J Surg Res* 114(2):133–139
- Cilla M, Pena E, Martinez M (2012) 3d computational parametric analysis of eccentric atheroma plaque: influence of axial and circumferential residual stresses. *Biomech Model Mechanobiol* 11(7):1001–1013
- Creane A, Maher E, Sultan S, Hynes N, Kelly DJ, Lally C (2010) Finite element modelling of diseased carotid bifurcations generated from in vivo computerised tomographic angiography. *Comput Biol Med* 40(4):419–429
- Cui F, Han HC, Zhang YW (2010) Mechanical performance study of vascular stent using computational modeling and simulation 6th world congress of biomechanics (WCB 2010). August 1–6, 2010 Singapore, IFMBE proceedings, vol 31. Springer, Berlin, pp 1443–1446
- Davis JR (2004) Tensile testing. ASM International, Materials Park
- Delfino A, Stergiopoulos N, Moore JE, Meister JJ (1997) Residual strain effects on the stress field in a thick wall finite element model of the human carotid bifurcation. *J Biomech* 30(8):777–786
- Di Martino E, Mantero S, Inzoli F, Melissano G, Astore D, Chiesa R, Fumero R (1998) Biomechanics of abdominal aortic aneurysm in the presence of endoluminal thrombus: experimental characterisation and structural static computational analysis. *Eur J Vasc Endovasc Surg* 15(4):290–299
- Franquet A, Avril S, Le Riche R, Badel P (2011) Identification of heterogeneous elastic properties in stenosed arteries: a numerical plane strain study. *Comput Methods Biomech Biomed Eng* 15(1):49–58
- Gao H, Long Q, Graves M, Gillard JH, Li ZY (2009) Carotid arterial plaque stress analysis using fluid-structure interactive simulation based on in-vivo magnetic resonance images of four patients. *J Biomech* 42(10):1416–1423
- Gasser TC, Ogden RW, Holzapfel GA (2006) Hyperelastic modelling of arterial layers with distributed collagen fibre orientations. *J R Soc Interface* 3(6):15–35
- Guinea GV, Atienza JM, Rojo FJ, Garciaa-Herrera CM, Yiquan L, Claes E, Goicolea JM, Garciaa-Montero C, Burgos RL, Goicolea FJ, Elices M (2010) Factors influencing the mechanical behaviour of healthy human descending thoracic aorta. *Physiol Meas* 31(12):1553–1565

- 579 Guyton A (1991) Textbook of medical physiology, 8th edn. W.B. Saunders, Philadelphia 630
- 580 631
- 581 Hanuza J, Maczka M, Gasior-Glogowska M, Komorowska M, 632
- 582 Kobielarz M, Bedzinski R, Szotek S, Maksymowicz K, Hermanowicz K (2010) Ft-raman spectroscopic study of thoracic aortic wall 633
- 583 subjected to uniaxial stress. *J Raman Spectrosc* 41(10):1163–1169 634
- 584 635
- 585 Herisson F, Heymann MF, Chetiveaux M, Charrier C, Battaglia S, Pilet 636
- 586 P, Rouillon T, Krempf M, Lemarchand P, Heymann D, Goueffic Y 637
- 587 (2011) Carotid and femoral atherosclerotic plaques show different 638
- 588 morphology. *Atherosclerosis* 216(2):348–354 639
- 589 640
- 590 Hollenstein M, Ehret A, Itskov M, Mazza E (2011) A novel experimental 641
- 591 procedure based on pure shear testing of dermatome-cut samples 642
- 592 applied to porcine skin. *Biomech Model Mechanobiol* 10(5):651– 643
- 593 661 644
- 594 Holzapfel G, Gasser T, Ogden R (2000) A new constitutive framework 645
- 595 for arterial wall mechanics and a comparative study of material models. *J Elast* 61(1):1–48 646
- 596 647
- 597 Holzapfel GA, Sommer G, Regitnig P (2004) Anisotropic mechanical 648
- 598 properties of tissue components in human atherosclerotic plaques. *J 649*
- 599 *Biomech Eng* 126(5):657–665, research support, Non-US Gov't, In 650
- 600 *Vitro* 651
- 601 Huang H, Virmani R, Younis H, Burke AP, Kamm RD, Lee RT 652
- 602 (2001) The impact of calcification on the biomechanical stability 653
- 603 of atherosclerotic plaques. *Circulation* 103(8):1051–1056 654
- 604 655
- 605 Kioussis DE, Rubinigg SF, Auer M, Holzapfel GA (2009) A methodol- 656
- 606 ogy to analyze changes in lipid core and calcification onto fibrous 657
- 607 cap vulnerability: the human atherosclerotic carotid bifurcation as 658
- 608 an illustratory example. *J Biomech Eng* 131(12):121,002 659
- 609 660
- 610 Krejza J, Arkuszewski M, Kasner SE, Weigele J, Ustymowicz A, Hurst 661
- 611 RW, Cucchiara BL, Messe SR (2006) Carotid artery diameter in 662
- 612 men and women and the relation to body and neck size. *Stroke* 663
- 613 37(4):1103–1105 664
- 614 665
- 615 Lally C, Reid AJ, Prendergast PJ (2004) Elastic behavior of porcine 666
- 616 coronary artery tissue under uniaxial and equibiaxial tension. *Ann 667*
- 617 *Biomed Eng* 32(10):1355–1364 668
- 618 669
- 619 Lawlor MG, O'Donnell MR, O'Connell BM, Walsh MT (2011) Exper- 670
- 620 imental determination of circumferential properties of fresh carotid 671
- 621 artery plaques. *J Biomech* 44(9):1709–1715 672
- 622 673
- 623 Lendon CL, Davies MJ, Richardson PD, Born GVR (1993) Testing 674
- 624 of small connective tissue specimens for the determination of the 675
- 625 mechanical behaviour of atherosclerotic plaques. *J Biomed Eng* 676
- 626 15(1):27–33 677
- 627 678
- 628 Li ZY, Tang T, U-King-Im J, Graves M, Sutcliffe M, Gillard JH (2008) 679
- 629 Assessment of carotid plaque vulnerability using structural and geometrical determinants. *Circ J Off J Jpn Circ Soc* 72(7):1092–1099
- 630 631
- 632 Loree HM, Grodzinsky AJ, Park SY, Gibson LJ, Lee RT (1994a) Static 633
- 634 circumferential tangential modulus of human atherosclerotic tissue. 635
- 636 *J Biomech* 27(2):195–204 637
- 638 639
- 640 Loree HM, Tobias BJ, Gibson LJ, Kamm RD, Small DM, Lee RT 641
- 642 (1994b) Mechanical properties of model atherosclerotic lesion lipid 643
- 644 pools. *Arterioscler Thromb Vasc Biol* 14(2):230–234 645
- 646 647
- 648 Maher E, Creane A, Sultan S, Hynes N, Lally C, Kelly DJ (2009) Tensile 649
- 650 and compressive properties of fresh human carotid atherosclerotic 651
- 652 plaques. *J Biomech* 42(16):2760–2767 653
- 654 655
- 656 Medtech-Insight (2011) US markets for peripheral vascular stents 657
- 658 report. Technical report 254, Medtech insight 659
- 660 661
- 662 Palmieri G, Chiappini G, Sasso M, Papalini S (2009) Hyperelastic materials 663
- 664 characterization by planar tension tests and full-field strain measurement. *Annu Conf Soc Exp Mech* 1:1–4 665
- 666 667
- 668 Paraskevas KI, Mikhailidis DP, Veith FJ (2009) Carotid artery stenting 669
- 670 may be losing the battle against carotid endarterectomy for the management 671
- 672 of symptomatic carotid artery stenosis, but the jury is still 673
- 674 out. *Vascular* 17(4):183–189 675
- 676 677
- 678 Raghavan M, Webster M, Vorp D (1996) Ex vivo biomechanical behavior 679
- 680 of abdominal aortic aneurysm: assessment using a new mathematical model. *Ann Biomed Eng* 24(5):573–582 681
- 682 683
- 684 Richardson PD (2002) Biomechanics of plaque rupture: progress, problems, 685
- 686 and new frontiers. *Ann Biomed Eng* 30(4):524–536 687
- 688 689
- 690 Roffi M, Mukherjee D, Clair DG (2009) Carotid artery stenting vs. 691
- 692 endarterectomy. *Eur Heart J* 30(22):2693–2704 693
- 694 695
- 696 Scherer S, Treichel T, Ritter N, Triebel G, Drossel W, Burgert O (2011) 697
- 698 Surgical stent planning: simulation parameter study for models based 699
- 700 on dicom standards. *Int J Comput Assist Radiol Surg* 6(3):319–327 701
- 702 703
- 704 Silver FH, Snowhill PB, Foran DJ (2003) Mechanical behavior of vessel 705
- 706 wall: a comparative study of aorta, vena cava, and carotid artery. *Ann 707*
- 708 *Biomed Eng* 31(7):793–803 709
- 710 711
- 712 Stemper BD, Yoganandan N, Pintar FA (2005) Methodology to study 713
- 714 intimal failure mechanics in human internal carotid arteries. *J Biomech* 715
- 716 38(12):2491–2496 717
- 718 719
- 720 Takashima K, Kitou T, Mori K, Ikeuchi K (2007) Simulation and exper- 721
- 722 imental observation of contact conditions between stents and artery 723
- 724 models. *Med Eng Phys* 29(3):326–335 725
- 726 727
- 728 Teng Z, Tang D, Zheng J, Woodard PK, Hoffman AH (2009) An exper- 729
- 730 imental study on the ultimate strength of the adventitia and media of 731
- 732 human atherosclerotic carotid arteries in circumferential and axial 733
- 734 directions. *J Biomech* 42(15):2535–2539 735
- 736 737
- 738 Veronda DR, Westmann RA (1970) Mechanical characterization of skin 739
- 740 finite deformations. *J Biomech* 3(1):111–124 741
- 742 743
- 744 Versluis A, Bank A, Douglas WH (2006) Fatigue and plaque rupture in 745
- 746 myocardial infarction. *J Biomech* 39(2):339–347 747
- 748 749
- 750 Wang DH, Makaroun M, Webster MW, Vorp DA (2001) Mechanical 751
- 752 properties and microstructure of intraluminal thrombus from abdominal 753
- 754 aortic aneurysm. *J Biomech Eng* 123(6):536–539 755
- 756 757
- 758 Xiong J, Wang SM, Zhou W, Wu JG (2008) Measurement and analysis 759
- 760 of ultimate mechanical properties, stress-strain curve fit, and elastic 761
- 762 modulus formula of human abdominal aortic aneurysm and non- 763
- 764 aneurysmal abdominal aorta. *J Vasc Surg* 48(1):189–195 765
- 766 767